

See discussions, stats, and author profiles for this publication at: <https://www.researchgate.net/publication/229923488>

Fracture analysis of strength undermatched Al-Alloy welds in edge cracked tensile panels using FITNET procedure

Article in *Fatigue & Fracture of Engineering Materials & Structures* · September 2008

DOI: 10.1111/j.1460-2695.2008.01260.x

CITATIONS

11

READS

97

3 authors:



Sergio Cicero

Universidad de Cantabria

212 PUBLICATIONS 832 CITATIONS

[SEE PROFILE](#)



Çınar Yeni

Dokuz Eylül University

30 PUBLICATIONS 300 CITATIONS

[SEE PROFILE](#)



M. Koçak

Gedik Holding, Gedik University

186 PUBLICATIONS 2,965 CITATIONS

[SEE PROFILE](#)

Some of the authors of this publication are also working on these related projects:



Análisis del comportamiento en fractura de componentes estructurales con defectos en condiciones de bajo confinamiento tensional (MAT2014-58443-P) [View project](#)



Spanish Network on Notch Mechanics (Red Española de Mecánica de Entallas) [View project](#)

Fracture Analysis of Strength Undermatched Al-Alloy Welds in Edge Cracked Tensile Panels Using FITNET Procedure

S. Cicero ⁽¹⁾, Ç. Yeni ⁽²⁾, M. Koçak ⁽³⁾

(1) University of Cantabria, ETS Ingenieros de Caminos, Canales y Puertos
Department of Materials Science and Engineering
Av. Los Castros s/n, 39005, Santander, Spain
(Corresponding author, fax nr: +34 942 201818, e-mail: ciceros@unican.es)

(2) Dokuz Eylul University, Faculty of Engineering, 35100, Bornova, Izmir, Turkey

(3) GKSS Research Center, Institute for Materials Research
Department of Joining and Assessment (WMF)
Max-Planck-Str. 1, D-21502 Geesthacht, Germany

ABSTRACT

This paper presents a methodology for the assessment of the remaining load carrying capacity of thin-walled components under tension containing highly strength undermatched welds and edge cracks. The analysis is based on the strength Mismatch Option of the Fracture Module, being a part of the newly developed European fitness-for-service (FFS) procedure FITNET. The Mismatch Option of the FITNET Fracture Module allows taking into account weld features like the weld tensile properties and weld geometry in the fracture analysis of cracked welded components. The methodology described was verified for centre cracked Al-alloy large tensile panels containing undermatched welds in Ref.1¹ and hence present work now provides validation with experimental results of the Single Edge Cracked (SEC) and Double Edge Cracked (DEC) Panels. The material used is an age-hardening aluminium alloy 6013 in T6 temper condition used in welded airframe components. The welds in the form of butt joints were produced using the CO₂ laser beam welding process. The results have shown that using the FITNET FFS methodology with appropriate selection of the input parameters, safe acceptable predictions of the maximum load carrying capacity of the welded panels can be obtained. It is also important to notice that one of the main difficulties that engineers find when applying mismatch analysis for first time is its apparent complexity. A step by step

analysis is here proposed with the intention of providing guidance for this kind of assessments.

KEYWORDS

FITNET, Single Edge Crack (SEC), Double Edge Crack (DEC), undermatch, laser beam welding, aluminium alloys

NOMENCLATURE

a	crack length for SEC specimen, half crack length for DEC specimen (mm)
A	elongation at fracture (%)
B	specimen thickness (mm)
A, B, C, A ₁ , B ₁ , C ₁ , A ₂ , B ₂ , C ₂	parameters in yield loci, Eq. 5, Eq. 9
E	modulus of elasticity (GPa)
f(L _r)	plasticity correction function, Eq. 20 - 21
f _m	parameter used for the calculation of yield loci, Eq. 7, Eq. 11
f _n	parameter used for the calculation of yield loci, Eq. 6, Eq. 10
F	externally applied load (kN)
F _Y	yield load (kN)
F _{YB}	yield load for base material (kN)
F _{YM}	mismatch corrected yield load solution (kN)
H	half weld width (mm)
K	elastic stress intensity factor (MPa \sqrt{m})
L _r	ratio of externally applied load to the yield load, Eq. 19
m	parameter for plane stress (m=1) and plane strain (m=2)
m [*]	parameter for normalizing the net section bending moment with respect to the plane stress yield load for uncracked base plates, Eq. 1, Eq. 8
M	mismatch factor defining the ratio between the weld and base metal yield strengths, Eq. 3
M _n	net section bending moment (Nm)
n [*]	parameter for normalizing the net section tensile force with respect to the plane stress yield load for uncracked all base plates, Eq. 1, Eq. 8
N _B	strain hardening exponent for base metal, Eq. 27
N _M	strain hardening exponent for mismatch, Eq. 26
N _n	net section tensile force (kN)
N _W	strain hardening exponent for weld metal, Eq. 28
Rp _{0.2}	(=σ _Y) yield strength (MPa)
W	total width for SEC specimen, half width for DEC specimen (mm)
β	parameter for calculation of the base metal yield load in case of a homogeneous DEC panel, Eq. 13
Δa	crack extension (mm)
Δa _{phy}	physical crack length (mm)
δ	crack tip opening displacement, CTOD (mm)
δ _e	elastic part of δ (mm)
δ ₅	CTOD; measured over a gauge length of 5 mm (mm)

ϕ	ratio of uncracked ligament length, (W-a), to the weld width , 2H, Eq. 2
χ	$\phi/10$, Eq. 12
μ_B	parameter used for calculation of $f(L_r)$, , Eq. 23
μ_M	parameter used for calculation of $f(L_r)$, , Eq. 22
μ_W	parameter used for calculation of $f(L_r)$, , Eq. 24
ν	Poisson's ratio
σ	applied stress (MPa)
σ_{YB}	yield strength of the base metal (MPa)
σ_{YW}	yield strength of the weld metal (MPa)
σ_{uts}	ultimate tensile strength (MPa)
$\sigma_{uts, B}$	ultimate tensile strength of the base metal (MPa)
$\sigma_{uts, W}$	ultimate tensile strength of the weld metal (MPa)
θ	yield loci, Eq. 4, Eq. 9
CDF	crack driving force
CT	compact tension type specimen
DEC	double edge crack
FAD	failure assessment diagram
FFS	fitness-for-service
FSW	friction stir welding
LBW	laser beam welding
SEC	single edge crack

INTRODUCTION

Driven by the demand for lighter and cost-effective airframes as well as by the close competition with the non-metallic composite materials, the design of metallic structures in the airframe fabrication has experienced revolutionary changes during the last decade. The well established joining technique by rivets is currently being replaced for some airframe applications by using novel welding technologies like laser beam welding (LBW) and friction stir welding (FSW). The adoption of these welding processes provides savings in structural weight and fabrication cost up to about 15%². It also reduces residual stresses on components due to the lower temperatures reached on the welding process. The most widely used metallic material in aircraft structures is aluminum alloy of 2xxx series and was considered to be unweldable³. However, newly developed aluminum alloys with silicon (Si) and magnesium (Mg) as the main alloying elements facilitate the use of low heat input welding technologies to manufacture crack and porosity free welds with good mechanical properties compared to the properties of the conventional base material alloys of 2xxx series¹.

Stringer-to-skin joints in some advanced airframes are already being produced using LBW with the use of high Si containing wire, whereas for the skin-to-skin joints, LBW and FSW techniques are currently under consideration in order to replace conventional riveted lap joints.

Current metallic airframes of airplanes are designed to satisfy the damage tolerance requirements in terms of fatigue and residual strength. The residual strength of a component is defined as the remaining load carrying capacity in presence of one or multiple cracks. Conventional analysis tools for the residual strength prediction of riveted thin-walled structures are well established. However, the move from the differential (riveted) to integral (welded) design of the airframe components introduces new aspects, which potentially need to be considered in the analysis route for cracked welded components made of thin sheets. The material is no longer homogeneous since joining of aluminium alloys by LBW and FSW usually produces a weld joint area having lower strength (undermatching) than the base material. In such welded structures, a lower strength weld zone leads to a localization of the plastic strain if the component experiences a high level of external loads and this can be significant particularly for the weld zone that has the same thickness as base metal. In particular, for cracks located in the weld material of the butt joints, the plastic zone at the crack tip can entirely be confined to the softer weld material leading to an increase of the crack tip constraint, which in turn may influence the fracture performance of the welded component. Such a development can partly be prevented by adequate design of the weld joint. However, it is essential to consider the material heterogeneity when structural integrity assessment needs to be conducted for cracks in the vicinity of such welds.

The identification of adequate input parameters based on the experimental observation of the deformation and damage process in the weld area is essential to describe the critical condition of strength undermatched structures. The selection of the strength and fracture toughness properties to be used in the FFS analysis (base material, welding or mismatched properties) of welded thin-walled structures has significant implications on the results. Currently, FITNET FFS procedure⁴ is providing an analysis route for the assessment of heterogeneous welds in thin-walled structures. Therefore, this paper aims at providing a validated procedure to assess the structural significance of flaws in strength undermatched LBW welds in thin Al-alloy sheets, continuing the work developed in Ref.1 for LBW and FSW welds in centre cracked tensile panels.

Deformation Characteristics of Highly Strength Undermatched Welds

The material investigated within this work is an age-hardening Al-alloy 6013 in T6 temper condition with the sheet thickness of 3.2 mm. The laser beam welding has been carried out using a single CO₂ laser source with an AlSi12 filler wire. The optical macro-section of the LBW butt joint is shown in Fig. 1. No post weld heat treatment has been applied to the welds. The welding process produced, as expected, strength undermatched welds (i.e. weld having lower yield strength than base metal). The Vickers micro-hardness profiles for the LBW joints are shown in Fig. 2, which clearly demonstrates the loss of strength in the weld area.

A detailed knowledge on the evolution of the plastic deformation at the crack tip in mismatched structures is essential to develop a methodology to assess its structural significance. For this purpose, a detailed investigation was conducted in Ref.1 on similar welds by using the experimental image analysis of the ARAMIS system⁵. ARAMIS is a correlation based image evaluation technique to capture the deformation distribution of a sample under load. The sample is viewed by a CCD camera, which records the surface

deformation in the form of digital images. The system then enables the calculation of the surface displacement and surface strain fields at each deformation step.

Based on the results obtained in Ref.1, it can be assumed that the plastic deformation is entirely confined to the lower yield strength weld material and does not penetrate into the base material. This is important to be defined for the selection of input data for the FITNET analysis. Although the plastic zone is confined to the weld material, base material properties are also necessary because they define the level of constraint for the yield loci allowing (or not) the plastic zone to take place also on the base material.

Weld Strength Mismatch Phenomenon

The yield load of a cracked component is defined as the load level at which the uncracked ligament starts yielding. **For the simple case of a homogeneous SEC panel** in combined bending and tension with a total width W , thickness B and the crack length a , the net-section bending moment and tensile force (Fig.3), M_n and N_n , are normalized with respect to the plane stress yield loads for uncracked all base plates⁶,

$$m^* \equiv \frac{4M_n}{\sigma_{YB}(W-a)^2} \quad ; \quad n^* \equiv \frac{N_n}{\sigma_{YB}(W-a)} \quad (1)$$

where σ_{YB} is the yield strength of the material. The mismatch yield loads are presented in the form of the yield loci $\Phi(m^*, n^*, M, \psi)$ where,

$$\psi = \frac{W-a}{H} \quad (2)$$

defines the ratio of the uncracked ligament length, $W-a$, and the weld width, $2H$, and,

$$M = \frac{\sigma_{YW}}{\sigma_{YB}} \quad (3)$$

is the mismatch factor defining the ratio between the weld (σ_{YW}) and base (σ_{YB}) material yield strengths. The general form of the yield loci is, for plane stress⁶:

$$\phi = \begin{cases} m^* + A \cdot n^{*2} + B \cdot n^* + C = 0 & \text{for } 0 \leq n^* \leq 0.974f_n \\ \frac{m^*}{f_m} + 12.735 \left(\frac{n^*}{f_n} - 1 \right) = 0 & \text{for } 0.974f_n \leq n^* \leq f_n \end{cases} \quad (4)$$

where,

$$A = \frac{1}{f_n} \left[1.7094 - 0.7051 \left(\frac{f_m}{f_n} \right) \right] ; B = -1.665 + 1.3735 \left(\frac{f_m}{f_n} \right) ; C = -f_m \quad (5)$$

The yield loci $\Phi=0$ in Eq.4 can be completely determined if f_m and f_n are known⁶. In the following the expressions for f_m and f_n are given for undermatching cases and assuming that yielding is confined within the weld material,

$$f_n = \begin{cases} M & \text{for } 0 \leq \psi \leq 1.43 \\ M \left(\frac{2}{\sqrt{3}} - \left(\frac{2-\sqrt{3}}{\sqrt{3}} \right) \frac{1.43}{\psi} \right) & \text{for } 1.43 \leq \psi \end{cases} \quad (6)$$

$$f_m = 1.072 \cdot M \quad (7)$$

For plane strain situations, the net-section bending moment and tensile force (Fig.3), M_n and N_n , are normalized with respect to the plane strain yield loads for uncracked all base plates⁶

$$m^* \equiv \frac{2\sqrt{3}M_n}{\sigma_{YB}(W-a)^2} \quad ; \quad n^* \equiv \frac{\sqrt{3}N_n}{2\sigma_{YB}(W-a)} \quad (8)$$

The general form of the yield loci is, for plane strain:

$$\phi = \begin{cases} m^* + A_1 \cdot n^{*2} + B_1 \cdot n^* + C_1 = 0 & \text{for } 0 \leq n^* \leq 0.55f_n \\ A_2 \left(\frac{m^*}{f_m} \right)^2 + B_2 \left(\frac{n^*}{f_n} - C_2 \right)^2 - 1 = 0 & \text{for } 0.55f_n \leq n^* \leq f_n \end{cases} \quad (9)$$

where,

$$\begin{aligned} A_1 &= \frac{1}{0.55f_n} \left[0.294 + \frac{1}{11} \left(\frac{f_m}{f_n} \right) \right] ; \quad B_1 = - \left[\frac{2}{11} \left(\frac{f_m}{f_n} \right) + 0.294 \right] ; \quad C_1 = -f_m \\ A_2 &= \frac{(0.55 - C_2)}{0.3087(1 - C_2)^2} \frac{f_m}{f_n} \quad ; \quad B_2 = \frac{1}{(1 - C_2)^2} \quad ; \quad C_2 = \frac{1.96f_m - 0.69f_n}{3.57f_m - 0.90f_n} \end{aligned} \quad (10)$$

Again, the yield loci $\Phi=0$ in Eq.9 can be completely determined if f_m and f_n are known. In the following the expressions for f_m and f_n are given for undermatching cases and assuming that yielding is confined within the weld material,

$$f_n = \begin{cases} M & \text{for } 0 \leq \psi \leq 1 \\ M \left(1.0 + 0.462 \frac{(\psi-1)^2}{\psi} - 0.044 \frac{(\psi-1)^3}{\psi} \right) & \text{for } 1 \leq \psi \leq 3.6 \\ M \left(2.571 - \frac{3.254}{\psi} \right) & \text{for } 3.6 \leq \psi \leq 5.0 \\ M \left(0.125\psi + 1.291 + \frac{0.019}{\psi} \right) & \text{for } 5.0 \leq \psi \end{cases} \quad (11)$$

$$f_m = \begin{cases} 1.2606M & \text{for } 0 \leq \psi \leq 2.0 \\ M(1.379 - 1.282\chi + 3.944\chi^2 - 2.461\chi^3) & \text{for } 2.0 \leq \psi \leq 7.0 \\ M(1.135 + 0.623\chi) & \text{for } 7.0 \leq \psi \end{cases} \quad \text{where } \chi = \frac{\psi}{10} \quad (12)$$

For the simple case of a homogeneous DEC (Fig. 4) panel with a total width $2W$, thickness B and the crack length $2a$, the yield load, F_{YB} , for plane stress conditions is given by Ref.4,

$$F_{YB} = \beta \cdot 2 \cdot \sigma_{YB} \cdot B \cdot (W - a) ; \quad \beta = \begin{cases} 1 + 0.54 \left(\frac{a}{W} \right) & \text{for } 0 \leq \frac{a}{W} \leq 0.286 \\ \frac{2}{\sqrt{3}} & \text{for } 0.286 \leq \frac{a}{W} \leq 1 \end{cases} \quad (13)$$

Then, the mismatch corrected yield load solution, F_{YM} , is,

$$F_{YM} = M \cdot F_{YB} \quad \text{for all } \psi \quad (14)$$

For plane strain conditions, the yield load is given by Ref.4,

$$F_{YB} = \beta \cdot \frac{4}{\sqrt{3}} \cdot \sigma_{YB} \cdot B \cdot (W - a) ; \quad \beta = \begin{cases} 1 + \ln \left(\frac{2W - a}{2(W - a)} \right) & \text{for } 0 \leq \frac{a}{W} \leq 0.884 \\ 1 + \frac{\pi}{2} & \text{for } 0.884 \leq \frac{a}{W} \leq 1 \end{cases} \quad (15)$$

Assuming that yielding occurs within the weld material, the mismatch corrected yield load solution, F_{YM} , is given by,

$$F_{YM} = \begin{cases} M \cdot F_{YB} & \text{for } 0 \leq \psi \leq 0.5 \\ \left[1 - (1 - M) \frac{0.5}{\psi} \right] \cdot F_{YB} & \text{for } 0.5 \leq \psi \end{cases} \quad (16)$$

The description of the weld strength mismatch as given above clearly indicates that an assessment of flaws in the vicinity of welds require a particular assessment procedure. This situation has been well practiced for strength overmatched steel or Ti-alloy welds. Flaws within the strength overmatched welds are principally protected. However, Al-alloy weldments generally show strength undermatching in varying degree depending on the alloy type and welding technology used. Contrary to the overmatched welds, flaws within the lower strength weld deposit will not be protected from applied strain by using inherent strength properties of the weld metal. Therefore, it is essential to provide additional shielding mechanisms for such flaws to promote damage tolerant behaviour. Development of efficient joint design and “local engineering” methods (e.g strengthening of the weld area) are required to overcome the loss of the load carrying capacity of such welds almost in all geometries.

METHODOLOGY AND APPROACH

The residual strength analysis of LBW wide plates is based on the Fracture Module of the FITNET FFS Procedure, which has been newly developed within a European thematic network FITNET^{4,8}. The procedure covers the failure (in four major areas: fracture, fatigue, creep, corrosion) analysis of metallic structures with and without welds giving clear guidelines for the evaluation of the structural significance of defects. The Fracture Module provides an engineering methodology for a prediction of critical conditions in terms of the maximum load or critical crack length in a cracked component. For the analysis of detected or postulated weld defects, the FITNET FFS Procedure provides a special analysis option. The FITNET FFS approach uses the methodology formerly known as the SINTAP procedure⁸ and

extends it with fully validated strength undermatched welded thin-walled structures. Therefore, present study aims to provide further verification of the FITNET FFS procedure using edge cracked thin-walled highly strength undermatched configurations. If the yield strength difference between the base and weld materials is more than 10%, the FITNET FFS Mismatch Option provides an assessment route accounting for the special features of welds, as it was established within the SINTAP procedure.

In the following, only the set of equations for the Mismatch Option of the Fracture Module will be given. For the complete information on the different analysis options within the FITNET FFS Procedure, the reader is referred to Ref.4. The required input information, as schematically illustrated in Fig. 5, for the application of the Fracture Module to cracked welded structures will be given subsequently, including the determination of the weld metal tensile and fracture properties. For the analysis of the strength mis-matched welds, the most important modification of the conventional structural integrity assessment routes was incorporation of the mis-match effect in the yield load. Hence numbers of mis-match corrected yield load solutions are compiled in the FITNET FFS Procedure, Annex B. It should be noted that mis-matched yield load solutions are strongly dependent on the strength mis-match ratio (M) and width (H) of the weld seam. Additionally, fracture toughness of the weld material is also strongly dependent on the strength mis-match ratio and notch location (i.e. weld centre or heat affected zone) since both parameters lead to changes in the crack tip local stresses (constraint) and hence it should experimentally be determined with great care.

FITNET FFS Procedure – Fracture Module,

Option 2: Weld Strength Mismatch

The Fracture Module provides two complementary analysis routes: Failure Assessment Diagram (FAD) and Crack Driving Force (CDF). Since both routes are based on the same set

of equations, they give identical results when the input data are treated identically. It is known that the basis of both routes is that failure is avoided as long as the welded structure is not loaded beyond its maximum load carrying capacity defined both fracture mechanics criteria and plastic limit analysis. The fracture mechanics analysis involves comparison of the loading on the crack tip (often called the crack tip driving force) with the ability of the material to resist cracking (defined by the material's fracture toughness or fracture resistance). The crack tip loading must be, in most cases, evaluated using elastic-plastic concepts and is dependent on the structure, the crack size and shape, the material's tensile properties and the loading. In the FAD approach, both the comparison of the crack tip driving force with the material's fracture toughness and the applied load with the plastic load limit are performed at the same time. In the CDF approach the crack driving force is plotted and compared directly with the material's fracture toughness. Separate analysis is carried out for the plastic limit analysis. Also, the CDF analysis provides information about the critical crack extension prior to failure. While both the FAD and CDF approaches are based on elastic-plastic concepts, their application is simplified by the use of elastic parameters together with plasticity corrections. The choice of approach is left to the user, and will depend upon user familiarity with the two different approaches and the analytical tools available. There is no technical advantage in using one approach over the other but the fact that, as said before, the CDF analysis can also predict the crack extension. Therefore, only the CDF route will be presented in detail in this paper, knowing that the FAD analysis would lead to identical results in terms of critical loads or crack sizes.

The CDF route requires calculation of the crack driving force on the cracked structure as a function of L_r . The crack driving force can be calculated in terms of J or crack tip opening displacement (CTOD), δ . Because the material fracture resistance will be provided in terms of CTOD δ_5 , it will be used the latter one, which is given as,

$$\delta = \delta_e [f(L_r)]^2 \quad (17)$$

with the elastic part of CTOD, δ_e ,

$$\delta_e = \frac{K^2}{m \sigma_Y E'} \quad (18)$$

K denotes the elastic stress intensity factor, the parameter m ($m=1$ for plane stress and $m=2$ for plane strain, as defined in Ref. 4,6 and 8) is considered a constraint parameter, $E'=E$ for plane stress and $E'=E/(1-\nu^2)$ for plane strain (E =Young's modulus, ν =Poisson's ratio), and,

$$L_r = \frac{F}{F_Y} \quad (19)$$

is the ratio of externally applied load, F , and the yield load, F_Y , of the cracked component which is a function of the material's yield strength, σ_Y , of the crack location and component/weld geometry. Regarding the selection of E' , the plane stress condition has been chosen due to the fact of the thin sheet material. It should be pointed out that for $\nu=0.3$, E' for the plane strain case differs only by a factor of 1.1 from the plane stress case, whereas the variation of m between 1 and 2 is much more pronounced. For the cases being analysed the value of m to be taken it is not straightforward because the plastic zone is confined to the weld material increasing the constraint conditions. This consideration is in opposition to the loss of constraint due to the small thickness of the specimens. For these reasons, the analysis here performed considers the two extreme possibilities of pure plane strain ($m=2$) and pure plane stress ($m=1$), knowing that the solution should be between them. The plasticity correction function, $f(L_r)$, is subdivided into different options within the FITNET FFS Procedure and is dependent on the extent of the material data input and on the case analyzed (homogeneous or heterogeneous with strength mismatch). For a strength mismatched

configuration (FITNET FFS Fracture Module Option 2), the plasticity correction function is defined as,

$$f(L_r) = \left[1 + \frac{1}{2}L_r\right]^{-1/2} \times [0.3 + 0.7\exp(-\mu_M L_r^6)] \quad \text{for} \quad 0 \leq L_r \leq 1 \quad (20)$$

$$f(L_r) = f(L_r = 1) \times L_r^{(N_M - 1)/2N_M} \quad \text{for} \quad 1 < L_r < L_r^{\max} \quad (21)$$

where,

$$\mu_M = \frac{M-1}{(F_{YM}/F_{YB} - 1)/\mu_W + (M - F_{YM}/F_{YB})/\mu_B} < 0.6 \quad \text{else} \quad \mu_M = 0.6 \quad (22)$$

$$\mu_B = 0.001 \frac{E}{\sigma_{YB}} < 0.6 \quad \text{else} \quad \mu_B = 0.6 \quad (23)$$

$$\mu_W = 0.001 \frac{E}{\sigma_{YW}} < 0.6 \quad \text{else} \quad \mu_W = 0.6 \quad (24)$$

$$L_r^{\max} = \frac{1}{2} \left(1 + \frac{0.3}{0.3 - N_M}\right). \quad (25)$$

Strain hardening exponents for mismatch, N_M , base, N_B , and weld materials, N_W , are defined as follows⁸⁻¹⁰,

$$N_M = \frac{M-1}{(F_{YM}/F_{YB} - 1)/N_W + (M - F_{YM}/F_{YB})/N_B} \quad (26)$$

$$N_B = 0.3 \left(1 - \frac{\sigma_{YB}}{\sigma_{UTS,B}}\right) \quad (27)$$

$$N_W = 0.3 \left(1 - \frac{\sigma_{YW}}{\sigma_{UTS,W}}\right). \quad (28)$$

σ_{UTS} denotes the ultimate tensile strengths of base (subscript B) and weld (subscript W) materials. F_{YM} and F_{YB} are the yield load solutions for the mismatch and base material plates, respectively.

By the use of Eq.26, the FITNET FFS procedure takes account of the interaction between base and weld metals in terms of post-yield properties of the weld joint constituents. The described procedure aims at reducing the excessive conservatism (in case of overmatching) and non-conservatism (in case of undermatching) in prediction of critical conditions for weld flaws. Also, there is a need for a fully validated procedure for undermatched welds in various configurations. The present study, therefore, focuses on the validation of this procedure for thin-walled highly strength undermatched Al-alloy welds.

Material Related Input Information

Tensile Properties

As mentioned in the previous section, one of the major input parameters in the analysis is the yield load of the mismatched configuration. The yield load solutions presented above contains the mismatch factor M , which in turn depends on the yield strength of the weld material. An important task is therefore the determination of the weld metal tensile properties. Two approaches can be followed: tensile tests using standard flat specimens containing transverse welds and micro-flat tensile specimens. In Ref.1, the convenience of using values from the latter was demonstrated.

Micro-flat tensile specimens enable the determination of local tensile properties in terms of full stress-strain curves. These 0.5 mm thick and 1.5 mm wide small specimens, Fig. 6, were extracted using electrical discharge machining (EDM) from different locations of the LBW joints. Fig. 6 also shows the extraction technique for sheet thicknesses up to about 3.0 mm.

For thicker plates, specimens can also be extracted across the weld joint. This technique yields full stress-strain curves obtained from the bulk material of the region of interest. The elongation was measured at a gauge length of $L_0 = 7$ mm. Special caution is needed in the definition of the notch radius of the specimens in order to avoid any notch effect on the static strength results of the material. It should be noted that micro-flat tensile specimens are made of all-weld material and thus provide the intrinsic (local) material tensile properties. Table 1 summarizes the tensile strength and elongation values for the materials obtained with the use of this technique. The high level of strength mis-match (44%) is readily visible in Table 1. It should be noted this information could not be obtained with the testing of conventional flat tensile specimens containing transverse welds.

Fracture Resistance

The widely used standard for the R-curve determination of the thin sheet material is ASTM E561¹¹ and is well established for the aerospace applications. However, the methodology given in this standard is only valid for homogeneous (unwelded) materials. The determination of the plasticity corrected effective crack length (Δa_{eff}), as required within this standard, is not transferable to welded configurations in a straight-forward manner. The plastic zone development at the tip of the crack within very narrow laser weld deposit is not similar to those of the homogeneous base metal crack. By using the ARAMIS method in Ref.1, the confined and elongated plastic zone development ahead of the crack tip located both at the weld centre and heat affected zone was demonstrated. Therefore, the standard methodology for the plastic zone size determination and hence the calculation of the effective crack extension for the cracks in strength mismatched welds needs to consider the mismatch factor (M) and the size of the weld ($2H$) as well as notch location. Moreover, the current FITNET FFS Procedure needs an R-curve in terms of a physical crack length (Δa_{phy}). The CTOD δ_5 approach¹² offers a method for the determination of the fracture resistance curves, which is

particularly suited for thin-walled structures. A specially designed clip is attached across (5.0 mm gauge length) the fatigue crack tip to measure the crack tip opening displacement as the crack stably advances during loading. It should be noted that standard CTOD determination using deeply notched ($a/W=0.5$) CT specimens is not possible for the thin plates since they do not fulfil the size requirements of the test standards. The use of initiation fracture toughness of the weld metal is the usual approach in FITNET FFS analysis. However, benefit occurs when the component and defect dimensions, such as crack size, wall thickness and remaining ligament, are much greater than the amount of ductile tearing being considered. Therefore, in this study, the analysis of defect in thin-walled Al-alloy weldments of large aerospace panels is considered which led the use of ductile tearing property of the weld metal.

Fig. 7 shows the fracture resistance curve in terms of CTOD δ_5 obtained for the LBW joints from the CT50 specimens with $a/W=0.5$ using the multiple specimen technique. Anti-buckling guides were used to ensure the Mode I type loading during the testing.

Component Related Input Data

K-factor Solution

The K -factors for SEC and DEC panels are available in Refs.4 and 13,

$$K_{I,SEC} = \frac{\sqrt{\pi} \left(1 + 2 \frac{a}{W}\right)}{\left(1 - \frac{a}{W}\right)^{3/2}} \left[1.12 - 3.68 \left(\frac{a}{W}\right) + 11.95 \left(\frac{a}{W}\right)^2 - 25.85 \left(\frac{a}{W}\right)^3 + 33.09 \left(\frac{a}{W}\right)^4 - 22.44 \left(\frac{a}{W}\right)^5 + 6.17 \left(\frac{a}{W}\right)^6 \right] \sigma \sqrt{a} \quad (29)$$

$$K_{I,DEC} = \frac{\sqrt{\pi}}{\left(1 - \frac{a}{W}\right)^{1/2}} \left[1.122 \left(1 - 0.5 \left(\frac{a}{W}\right)\right) - 0.015 \left(\frac{a}{W}\right)^2 + 0.09 \left(\frac{a}{W}\right)^3 \right] \sigma \sqrt{a} \quad (30)$$

where σ is the applied stress, W is the total panel width in SEC panels and half the panel width in DEC panels, a is the crack length, and B is the panel thickness. It is important to notice that taking the panel thickness as B is a conservative judgment, as the weld bead is a bit larger along the entire weld. Since K is a purely geometrical function, it is also valid for heterogeneous configurations like welded panels.

Yield Load Solution

The second component related input parameter of the FITNET FFS flaw assessment procedure is the mismatch corrected yield load solution, F_{YM} , which has already been presented in the previous section and given in Eq.1 to 16.

Note that these solutions are only valid for highly undermatched welds where the plastic deformation at the crack tip located in the weld does not penetrate into the base material. This consideration is specifically applicable to LBW joints of 6xxx series Al-alloys.

FITNET Prediction of the Load Carrying Capacities of the Welded SEC and DEC Panels

The input information needed for the application of the FITNET FFS Procedure – Fracture Module (see Fig. 5) is presented in previous sections. Both SEC and DEC configurations were tested with two different crack lengths, $a/W=0.2$ and $a/W=0.5$, so that the validation process covers some variability of crack lengths. Multiple specimens were tested in most cases as shown in Table 2.

In the analysis of highly strength undermatched case as this paper deals with, it is important to consider the both plane stress and plane strain states, since the strength undermatching can

significantly affect the crack tip constraint condition. It should be noted that the strength mismatch effect is more significant for the plane strain condition than the plane stress regardless than the a/W . Furthermore, for a conservative approach the plane stress solution is preferable as the plane stress limit load is lower than that in plane strain and its use, therefore, leads to higher values of L_r . In practice, component behaviour may correspond to neither idealisation and both solutions can be used to demonstrate the sensitivity of the assessment to the choice of limit load solution.

The results of the assessments are shown in Figs. 8 – 11 both for plane stress and plane strain hypotheses. The dotted lines represent the extrapolation of the resistance curves to crack extensions where no experimental data were available and here, it is considered that they sufficiently represent the material fracture resistance. A great sensitivity on the results is observed regarding to these hypotheses. The comparison between experimental and analytical results is shown in Table 2 and Fig. 12. It can be observed that experimental results are generally between plane stress and plane strain solutions and closer to the first one, as it could be expected for thin-walled sheets. In $SEC_{a/W=0.5}$ panels, plane strain hypothesis gives better results than plane stress, being the latter over conservative. This could be caused by the high constraint conditions in the crack tip produced by the crack length (long crack) and the external forces (high bending component). During the precracking of one of the DEC panels, there was fatigue crack growth mainly on one of the notches, therefore, fracture process was controlled by the longer crack side and this panel was considered as a SEC specimen (see Table 2 for one test on $DEC_{a/W=0.2}$ and three tests on $SEC_{a/W=0.2}$). In all plane stress cases and in plane strain assessment for $SEC_{a/W=0.5}$, the instability point was reached within the range of the R-curve that has been covered during its determination with CT50 specimens. Therefore, no extrapolations needed to be performed, except for the two plane strain cases.

The results of the FITNET analysis with the use of plane stress condition have provided conservative predictions of the attained maximum loads for all specimen geometries. The repetition of the experiments has also secured the variability of the experimentally obtained maximum loads as shown in Fig. 12 and Table 2.

Furthermore, the results of the variation of the weld width, $2H$, and the strain hardening exponent, N_w , of the strength undermatched weld material have proven a minor influence on the FITNET FFS residual strength predictions and are reported elsewhere¹⁴.

Finally, the applicability of FITNET FFS Procedure Fracture Module to the analysis of flaws in highly strength undermatched advanced welds such as LBW of aerospace grade Al-alloy 6013 in thin-walled condition has been demonstrated. It has been shown that special care should be exercised in selecting the material input parameters and the assumption on the stress state of the panels.

CONCLUSIONS

The application of the mismatch Option of the Fracture Module of the FITNET FFS Procedure to LBW panels containing edge cracks has yielded conservative estimations of the maximum load carrying capacity when considering plane stress conditions. This analysis option allows for the account of weld specific features like the local tensile properties of the weld material as well as the weld geometry by including the weld width, $2H$, in the yield load solution of the strength mismatched configuration.

During the verification of the FITNET FFS Procedure for highly strength undermatched Al-alloy welds in thin-walled structures under tension yielded following results:

- The variation of selected input parameters has shown that the residual strength predictions are less sensitive to the weld width, $2H$, and the weld metal strain hardening exponent, N_w .
- It is recommended to determine and use local tensile properties of the weld material with micro-flat tensile specimens, as shown here and in Ref.1.
- The results obtained in the experiments are acceptably predicted by the FITNET FFS Procedure and are generally situated close to the plane stress prediction (due to the small thickness of the panels). Highly constrained situations (i.e, SEC panels with long cracks) plane stress hypothesis can lead to excessive conservatism. Also, a big part of the conservatism comes from considering the weld bead equal to the thickness of the panels, when actually, its thickness is larger. For example, looking to Fig. 1, the weld thickness is around 3.75 mm (and not 3.2). For this value, the critical load for DEC panel ($a/W=0.5$) in plane stress conditions would move from 50.8 kN to 59.5 kN (the experimental one is around 70 kN) and then, half of the conservatism would be eliminated. In case of $a/W=0.2$, the critical load for the DEC panel in plane stress conditions would change from 79.9 to 94.0 kN (the experimental one is 115.0 kN)

Finally, FITNET FFS Procedure offers an advanced flaw assessment methodology to the needs of the recent technological developments in the field of thin-walled laser welded structures (e.g. the airframe fabrication using welded metallic integral structures). Although, examples are taken from welded aerospace Al-alloys, the procedure has a generic nature and equally applicable to all welded thin walled strength undermatched welds.

ACKNOWLEDGEMENTS

Authors wish to thank Dr. J. Hackius, AIRBUS Bremen, and Dr. W. V. Vaidya, GKSS, for provision of welded material and mechanical data.

REFERENCES

1. Seib E, Koçak M (2005). *Fracture Analysis of Strength Undermatched Welds of Thin-Walled Aluminium Structures Using FITNET Procedure*. IIW Doc. X-1577-2005.
2. Rendigs K -H (1997). Aluminium Structures Used in Aerospace - Status and Prospects. *Materials Science Forum*. **242**: 11-24.
3. Irving B (1997). Why Aren't Airplanes Welded. *Welding Journal*. **76(1)**: 31-42, 1997.
4. FITNET, European Fitness-for-Service (FFS) Network. GIRT-CT-2001-05071, <http://www.eurofitnet.org> .
5. ARAMIS. Optical deformation analysis, <http://www.gom.com> .
6. Schwalbe K -H, Kim Y -J, Hao S, Cornec A, Koçak M (1997). *EFAM ETM-MM 96: The ETM Method for Assessing the Significance of Crack-Like Defects in Joints with Mechanical Heterogeneity (Strength Mismatch)*. GKSS Report 97/E/9, GKSS Forschungszentrum.
7. Koçak M (2005). *Fitness for Service Analysis of Structures Using FITNET Procedure: an Overview*. Proceedings of the 24th International Conference on Offshore Mechanics and Arctic Engineering (OMAE), Halkidiki, Greece.
8. SINTAP, Structural **IN**Tegrity **A**ssessment **P**rocedure, Final Revision. EU-Project BE 95-1462. Brite Euram Programme, 1999.
9. Ruiz Ocejó J, Gutiérrez-Solana F (1998). *On the Strain Hardening Exponent Definition and its Influence within SINTAP*, SINTAP Report UC/07, University of Cantabria.
10. Ruiz Ocejó J, Gutiérrez-Solana F (1998). *Validation of Different Estimations of N*. SINTAP Report UC/09, University of Cantabria.
11. ASTM E561. Standard Practice for R-curve Determination. Annual book of ASTM Standards, Vol. 03.01, 1994.
12. Schwalbe K -H (1995). Introduction of δ_5 as an Operational Definition of the CTOD and its Practical Use. *Fracture Mechanics*. **ASTM STP 1236**: pp. 763-778.
13. Al Laham S (1998). *Stress Intensity Factor and Limit Load Handbook*. SINTAP/Task 2.6, EPD/GEN/REP/0316/98.
14. Koçak M, Seib E, Motarjemi A (2005). *Improvements to the Fracture Assessment of Welds Using FITNET Fitness-for-service Assessment Procedure*. Proceedings of the 24th International Conference on Offshore Mechanics and Arctic Engineering (OMAE), Halkidiki, Greece.

Table 1 Material properties of the weld and base materials obtained from micro-flat tensile specimens.

Material	Yield strength $\sigma_Y=R_{p0.2}$ [MPa]	Tensile strength σ_{UTS} [MPa]	Elongation at fracture, A [%]	Mismatch factor, $M=\sigma_{YW}/\sigma_{YB}$ --
Micro-flat tensile specimens				
Base (LT)	330	365	11.5	
LBW (FZ)	145	165	2.0	0.44

Table 2 Comparison between experimental results and those obtained from the assessment under plane stress and plane strain conditions.

Geometry	Crack length (a/W)	Test	Max. Load, kN EXPERIMENT	Max. Load, kN FITNET FFS (PLANE STRESS)	Max. Load, kN FITNET FFS (PLANE STRAIN)
SEC	0.2	1	78.1	66.7	130.0
		2	74.8	66.7	130.0
		3	74.3	68.0	133.0
	0.5	1	34.7	18.8	29.4
		2	36.3	19.5	28.1
DEC	0.2	1	115.0	79.9	184.0
	0.5	1	69.1	50.8	114.0
		2	71.5	50.8	114.0

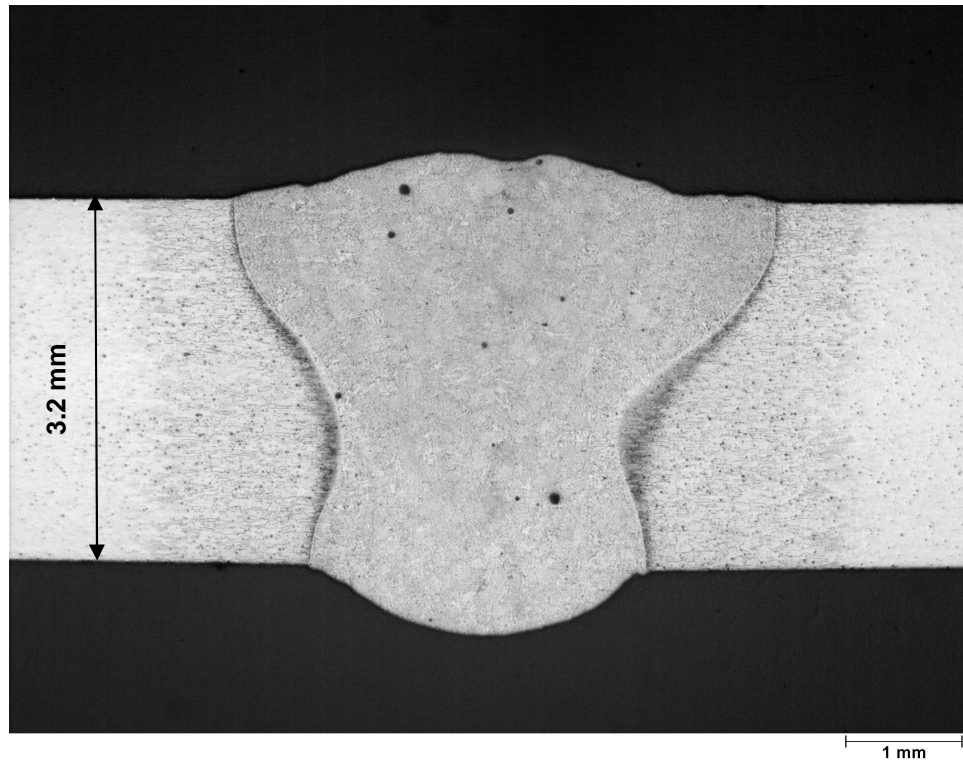


Fig. 1 Macro-section of a LBW butt joint

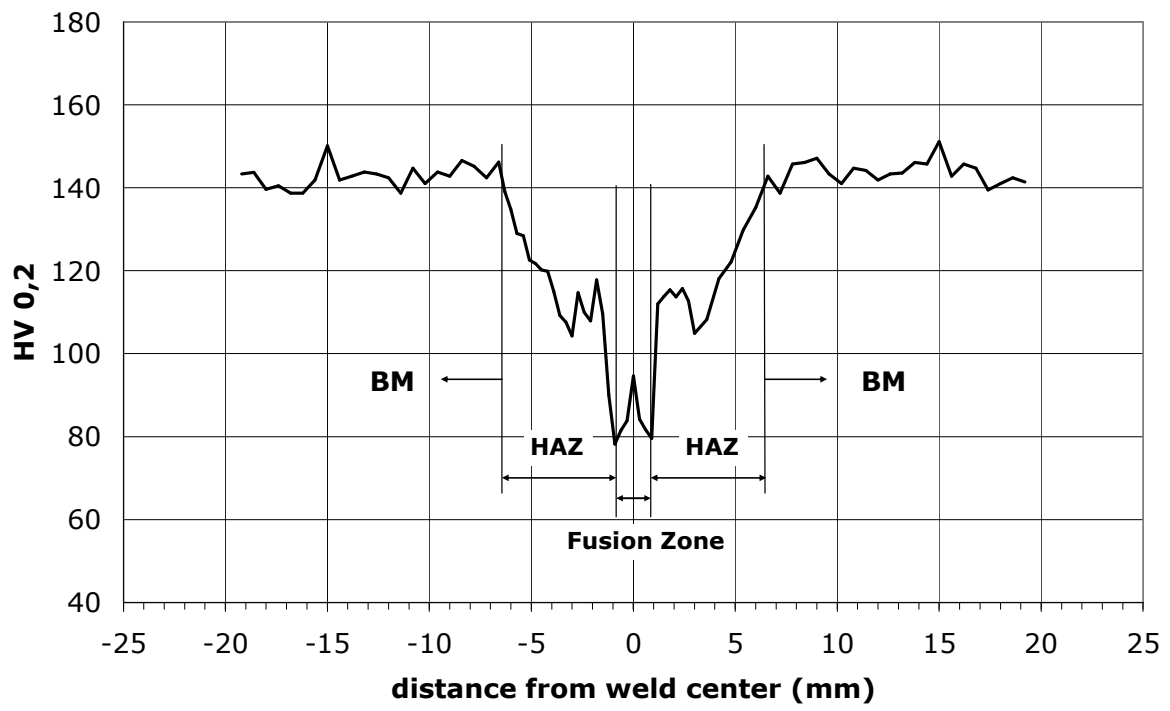


Fig.2 Micro-hardness profile of LBW butt joint

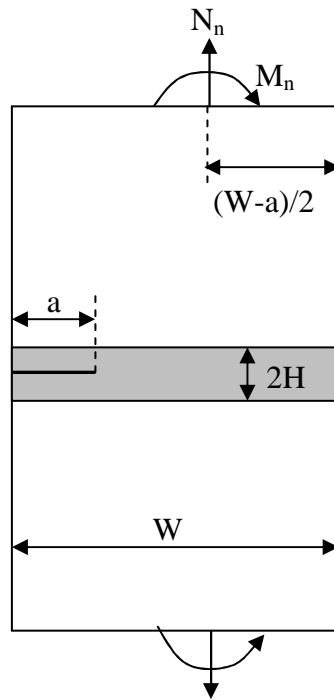


Fig.3 Definition of geometrical parameters for Single Edge Cracked (SEC) panels.

$W = 200 \text{ mm}$. $H = 2 \text{ mm}$

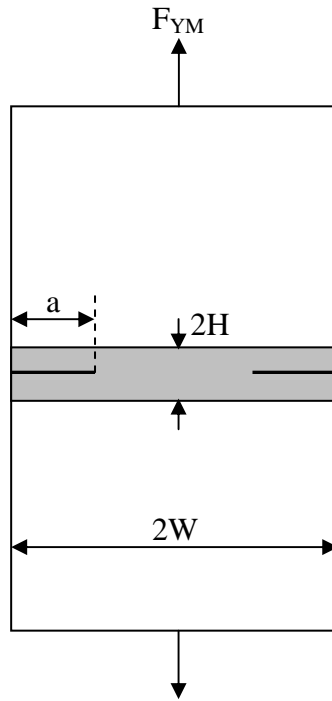


Fig.4 Definition of geometrical parameters for Double Edge Cracked (DEC) panels.

$$2W = 200 \text{ mm.}$$

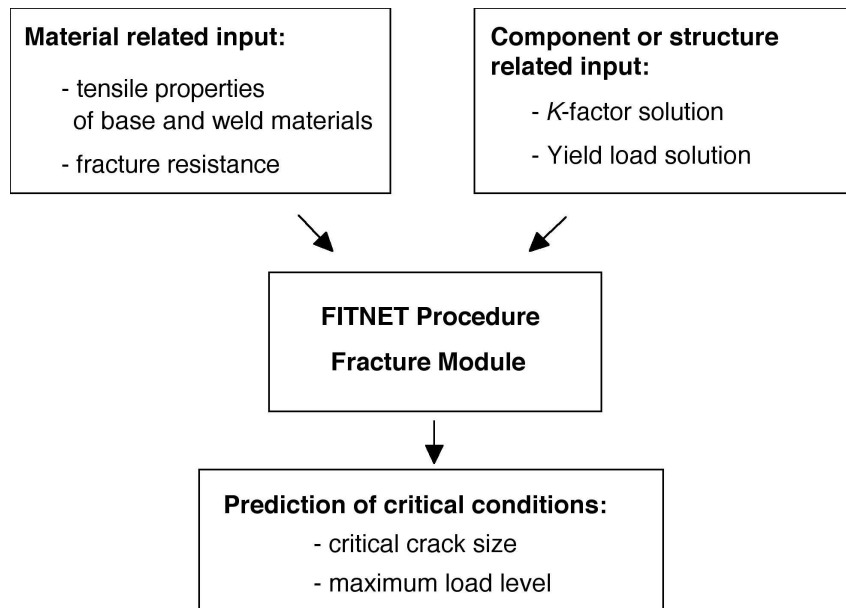


Fig.5 Required input information for the application of the FITNET FFS Procedure – Fracture Module for prediction of critical conditions (here, the critical condition considered has been the maximum load level).

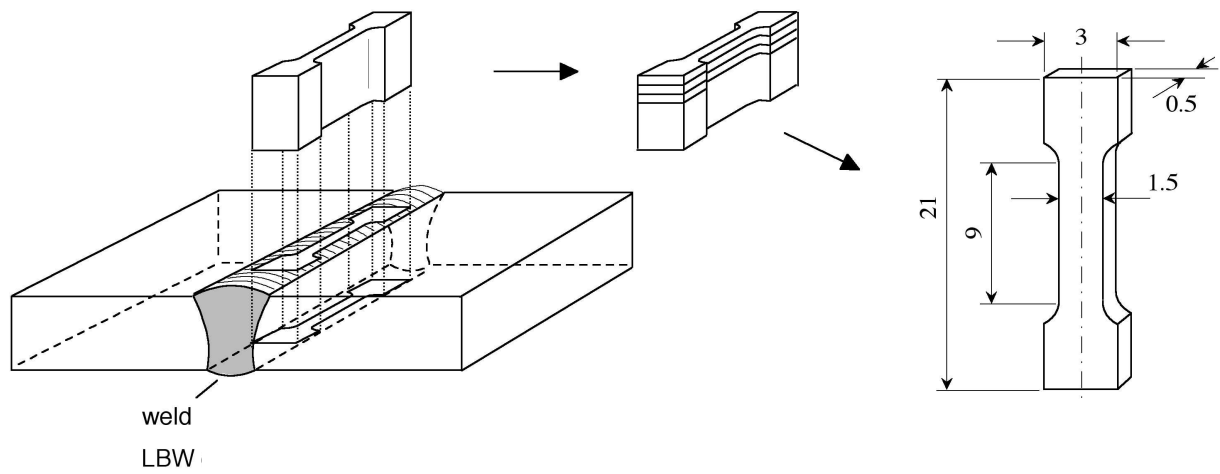


Fig.6 Schematics of the micro-flat tensile specimen extraction from the LBW welds. All dimensions are given in mm (Ref.1).

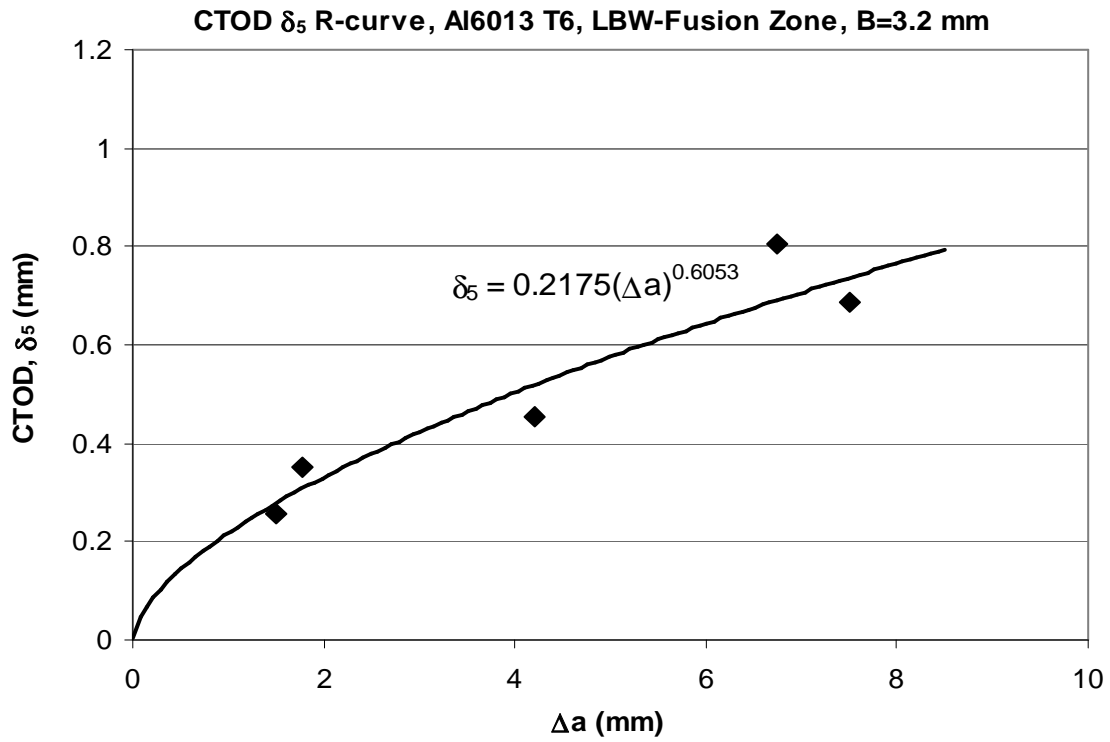
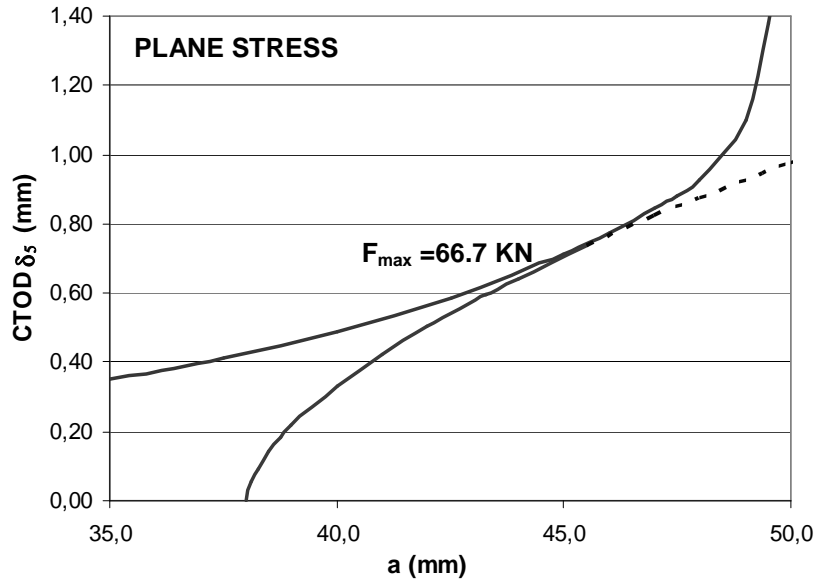


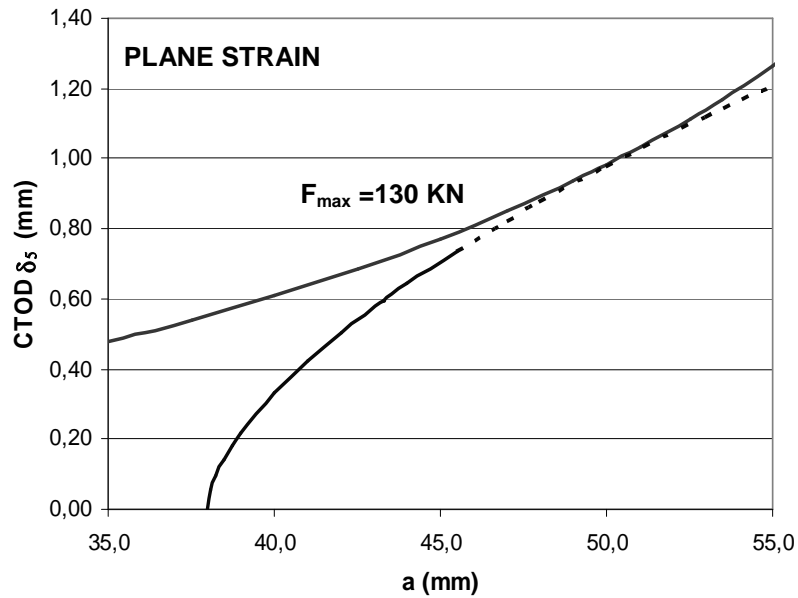
Fig.7 CTOD δ_5 R-curves for LBW (crack in fusion zone) welds obtained from the respective CT50 specimens

Al 6013 T6, SEC LBW, $a/W=0.2$, $B=3.2$ mm



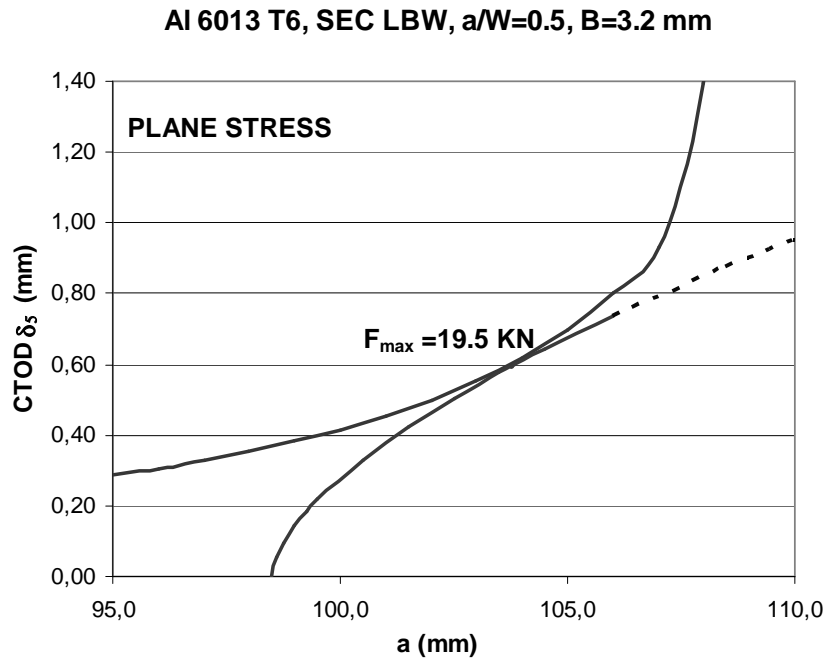
a)

Al 6013 T6, SEC LBW, $a/W=0.2$, $B=3.2$ mm

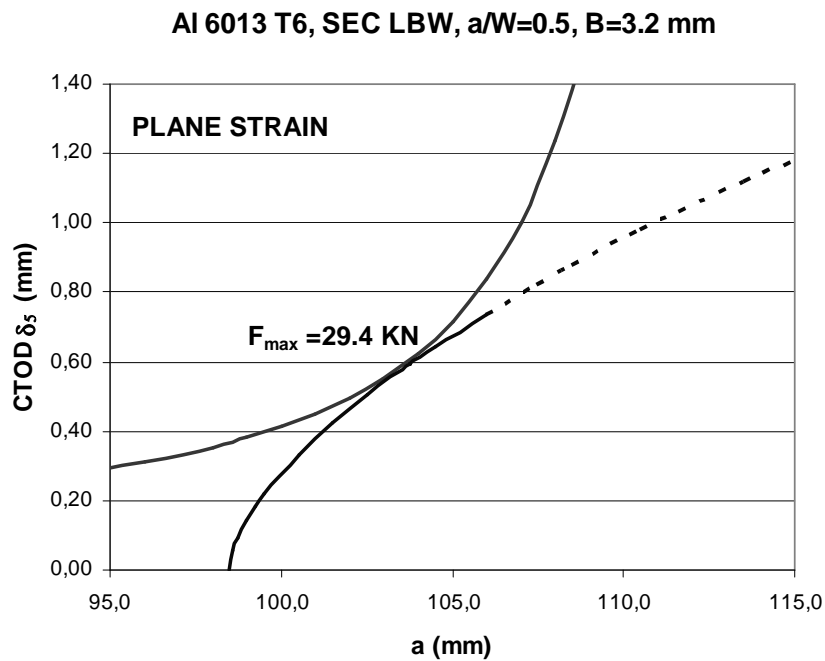


b)

Fig.8 Prediction of the maximum load carrying capacity of LBW SEC panels. $a/W=0.2$. Tests 1 and 2. a) Plane stress conditions; b) Plane strain conditions

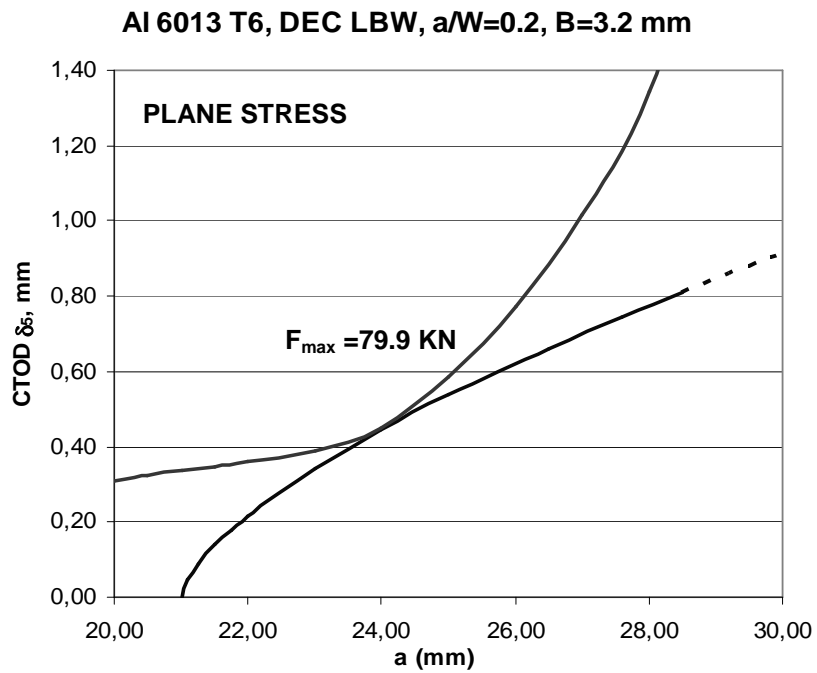


a)

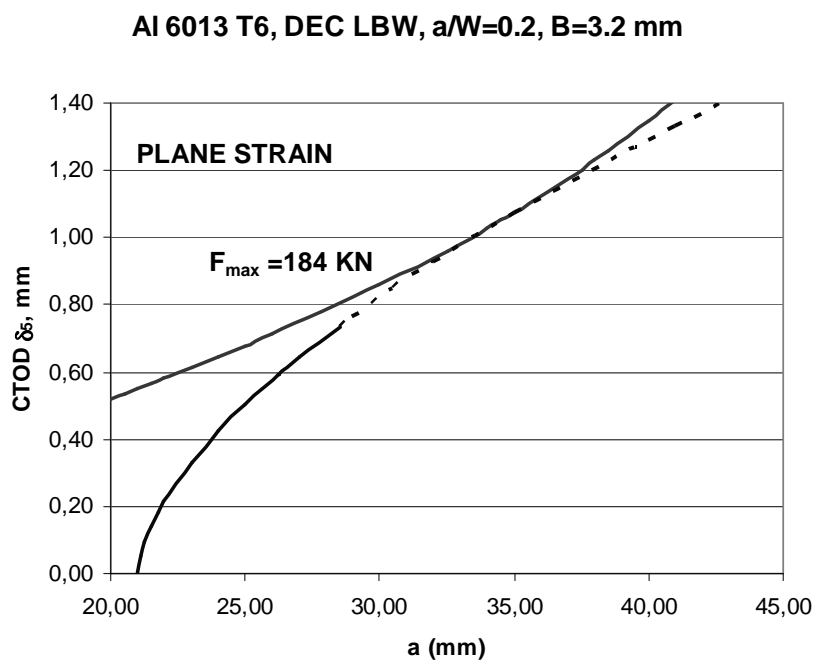


b)

Fig.9 Prediction of the maximum load carrying capacity of LBW SEC panels. $a/W=0.5$. Test 2. a) Plane stress conditions; b) Plane strain conditions



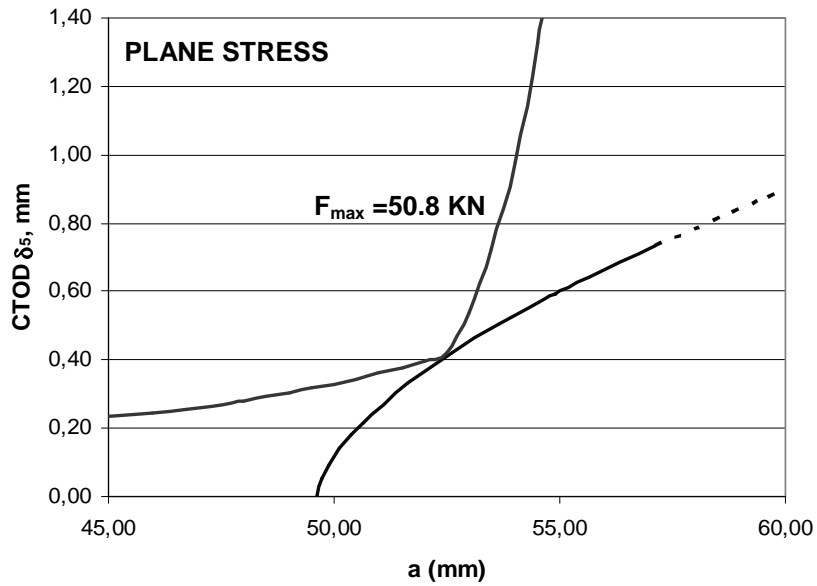
a)



b)

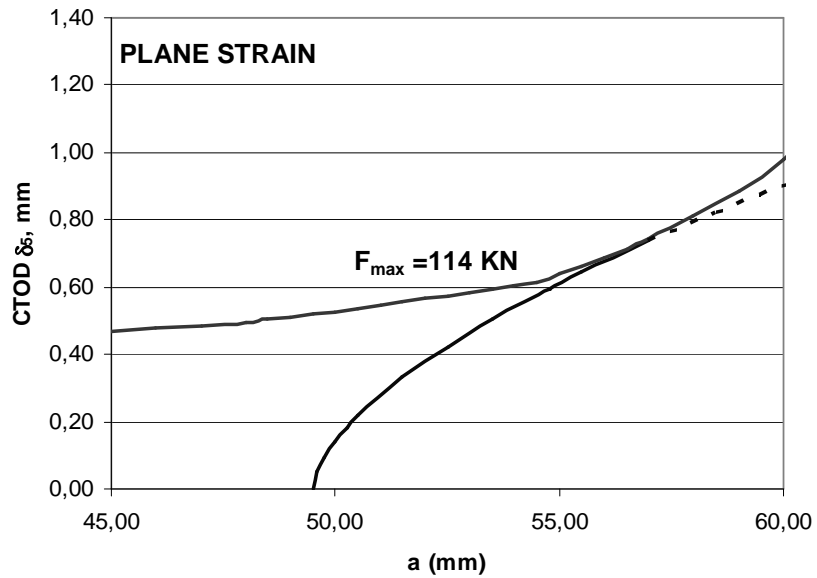
Fig.10 Prediction of the maximum load carrying capacity of LBW DEC panels. a/W=0.2, Test 1. a) Plane stress conditions; b) Plane strain conditions

Al 6013 T6, DEC LBW, a/W=0.5, B=3.2 mm



a)

Al 6013 T6, DEC LBW, a/W=0.5, B=3.2 mm



b)

Fig.11 Prediction of the maximum load carrying capacity of LBW DEC panels, a/W=0.5, Tests 1 and 2. a) Plane stress conditions. The observed “knee” is due to the change in the $f(Lr)$ definition for $1 \leq Lr \leq Lr_{max}$; b) Plane strain conditions

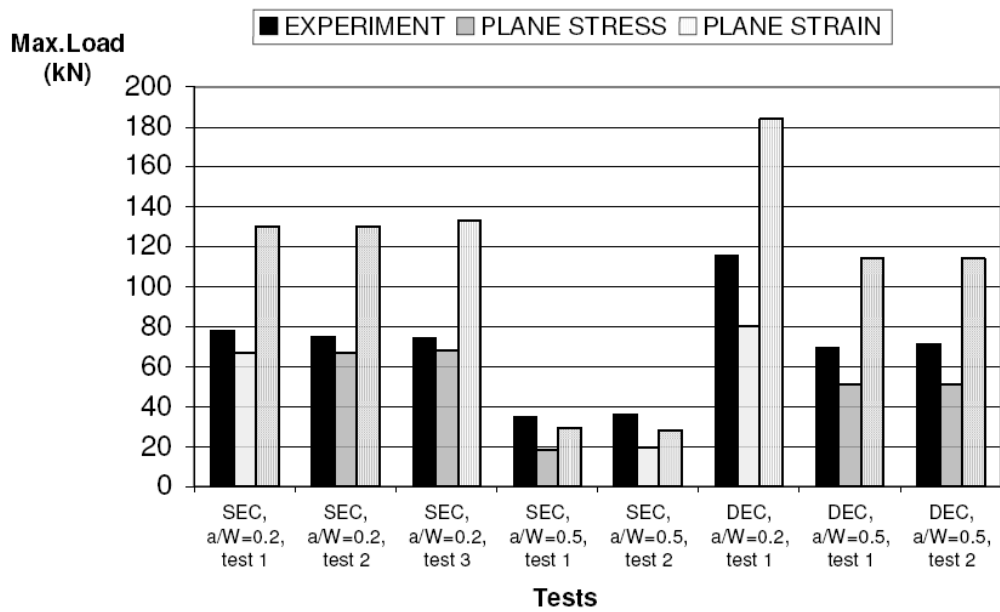


Fig.12 Comparison between experimental results and those obtained from the assessment under plane stress and plane strain conditions